

Storm Surge Clusters, Multi-Peak Storms and Their Effect on the Performance of the Maeslant Storm Surge Barrier (The Netherlands)

Bakker, Alexander M.R.; Rovers, Dion L.T.; Mooyaart, Leslie F.

DOI

[10.3390/jmse13020298](https://doi.org/10.3390/jmse13020298)

Publication date

2025

Document Version

Final published version

Published in

Journal of Marine Science and Engineering

Citation (APA)

Bakker, A. M. R., Rovers, D. L. T., & Mooyaart, L. F. (2025). Storm Surge Clusters, Multi-Peak Storms and Their Effect on the Performance of the Maeslant Storm Surge Barrier (The Netherlands). *Journal of Marine Science and Engineering*, 13(2), Article 298. <https://doi.org/10.3390/jmse13020298>

Important note

To cite this publication, please use the final published version (if applicable). Please check the document version above.

Copyright

Other than for strictly personal use, it is not permitted to download, forward or distribute the text or part of it, without the consent of the author(s) and/or copyright holder(s), unless the work is under an open content license such as Creative Commons.

Takedown policy

Please contact us and provide details if you believe this document breaches copyrights. We will remove access to the work immediately and investigate your claim.

Article

Storm Surge Clusters, Multi-Peak Storms and Their Effect on the Performance of the Maeslant Storm Surge Barrier (The Netherlands)

Alexander M. R. Bakker^{1,2,*} , Dion L. T. Rovers³ and Leslie F. Mooyaart^{1,2}

¹ Faculty of Civil Engineering and Geosciences, Delft University of Technology, Stevinweg 1, P.O. Box 5048, 2628 CN Delft, The Netherlands; l.f.mooyaart@tudelft.nl

² Rijkswaterstaat, Ministry of Infrastructure and Water Management, Griffioenlaan 2, P.O. Box 2232, 3526 LA Utrecht, The Netherlands

³ HKV Consultants, Informaticalaan 8, 2628 ZD Delft, The Netherlands; rovers@hkv.nl

* Correspondence: a.m.r.bakker@tudelft.nl

Abstract: Storm surge barriers are crucial for the flood protection of the Netherlands and other deltas. In the Netherlands, the reliability of flood defenses is typically assessed based on extreme water levels and wave height statistics. Yet, in the case of operated flood defenses, such as storm surge barriers, the temporal clustering of successive events may be just as important. This study investigates the evolution and associated flood risk of clusters of successive storm tide peaks at the Maeslant Storm Surge Barrier in the Netherlands. Two mechanisms are considered. Multi-peak storm surge events, as a consequence of tidal movement on top of the surge, are studied by means of stochastic storm tide events. Clusters of storm tides resulting from different, but related storms are investigated by means of time series analysis of a long sea-level record. We conclude that the tendency of extreme storm tide peaks to cluster is especially related to the seasonality in storm activity. In the current situation, the occurrence of clusters of storm tide peaks have only a minor influence of the flood risk in the area behind the Maeslant Storm Surge Barrier. We envision, however, that this influence is likely to increase with sea-level rise. The numbers are, however, uncertain due to the strong sensitivity to assumptions, model choices and the applied data set. More insight into the statistics of the time evolution of extreme sea water levels is needed to better understand and ultimately to reduce these uncertainties.



Academic Editor: Rafael J. Bergillos

Received: 17 December 2024

Revised: 27 January 2025

Accepted: 4 February 2025

Published: 6 February 2025

Citation: Bakker, A.M.R.; Rovers, D.L.T.; Mooyaart, L.F. Storm Surge Clusters, Multi-Peak Storms and Their Effect on the Performance of the Maeslant Storm Surge Barrier (The Netherlands). *J. Mar. Sci. Eng.* **2025**, *13*, 298. <https://doi.org/10.3390/jmse13020298>

Copyright: © 2025 by the authors. Licensee MDPI, Basel, Switzerland. This article is an open access article distributed under the terms and conditions of the Creative Commons Attribution (CC BY) license (<https://creativecommons.org/licenses/by/4.0/>).

Keywords: multi-peak storms; storm surge barrier; flood risk; storm surge clusters; operational reliability; storm surge barrier performance; Maeslant storm surge barrier; compound events

1. Introduction

Early in 2022, four severe storms (Corrie, Dudley, Eunice and Franklin) raged over the Netherlands, of which the latter three hit the Dutch coast in a time span of less than five days. The question is how well the Dutch flood protection system can deal with such a series of storms. Will there be enough time to recover from the previous storm?

Coastal flood risk assessments often focus on flooding caused by single extreme storm events [1,2]. Hydrological extremes in coastal areas can, however, also result from the simultaneous occurrence of two or more mildly extreme events [1,3,4] such as a prolonged period of high sea water levels in combination with enhanced precipitation [5] or the co-occurrence of storm surges together with high river discharges [6]. Therefore, there has been a growing interest in what are known as ‘compound drivers’ that together may lead to flooding or other disasters [1,4,7].

A temporary compound event is defined as a succession of multiple (either the same or different) hazards within a short time frame [3]. One example is a cluster of extreme sea level events over a relatively short time period. Two or more rapidly succeeding events may result in reduced time for repair and recovery, making the affected system more vulnerable [8–10]. For instance, a sequence of mildly extreme storm tides can cause similar dune erosion as a much extremer single storm tide event [2,11,12]. Likewise, Van den Brink and De Goederen [13] investigated two successive exceedances of the closure decision level of the Maeslant Storm Surge Barrier (the Netherlands), in such a short time span that there is insufficient time to fully recover from damage that occurred during the first closure.

Storm surge barriers (SSBs) play an important role in the flood protection of the Netherlands. Under normal conditions they are fully open to facilitate functions such as navigation, tidal exchange and ecological migration. Yet, during severe storm tides, they are closed to protect the hinterland against flooding [14]. Typically, strict standards for operational reliability are applied to safeguard a high protection level [15].

Shortly after a closing operation, operational reliability may temporarily deviate from the base reliability at the first closure [13,16]. On the one hand, a successful closure confirms that the SSB is in good condition and that its functionality is most likely not impacted by ‘dormant failures’ (dormant failures are failures of non-operating parts that cannot be observed without additional testing). This would imply a higher operational reliability shortly after a successful closure. On the other hand, however, even during successful operation, an SSB, and especially the Maeslant Storm Surge Barrier (MSSB), is susceptible to smaller and larger damage [13,16] which needs to be repaired for the barrier to become fully operational again. Depending on the type of damage, the repair may require considerable time. In the current situation, the maintenance of storm surge barriers can already be demanding [17,18] and, as a result of sea level rise, this may become even more challenging in future [19]. To assess the additional risk due to damage caused by the previous operation, it is important to gain insight into the probability of multiple successive storm tide peaks exceeding the closure decision level in a short time frame.

Multiple successive storm tide peaks exceeding the closure decision level of the Maeslant Storm Surge Barrier (MSSB) can originate from either the same storm surge event or from a cluster of multiple successive storm surge events. Storm tides are usually characterized by several distinct peaks [20]. During the low in between two peaks, it is sometimes necessary to open the SSB when the inner basin water level becomes higher than the sea water level. This negative head can be an opportunity to drain the inner basin during a prolonged period of high sea water levels, but can also be a threat to structural integrity since SSB’s are not always designed to withstand large negative heads. Either way, during an extreme storm surge event, there might be reason to temporarily open the barrier. In this study, we define a multi-closure event (MCE) as a storm surge event during which the SSB of interest needs to close (and open) twice or more. In contrast, we define a cluster of closure events (CCE) as a series of successive storm surge events within less than one month, during which the SSB needs to close at least once.

A storm tide is the sea water level during a storm surge event. The hydrograph (its temporal evolution) is mainly determined by astronomical tides, storm surges and their interplay [21,22]. Due to their strong dependence on astronomical forces, tides are well predictable and can therefore be considered a deterministic process [19,23], characterized by distinct subdaily, daily, monthly, seasonal and interannual variability [24]. Storm surges, on the other hand, are often considered a stochastic process [9] as they are mainly driven by near-surface wind and atmospheric pressure [25]. Along the Dutch coast, the most pronounced storm surges are found with northerly or northwesterly storms as these directions provide the longest wind fetch [5,13,26].

Storm surges and tides are subject to complex interactions [20,21,27] that may influence the storm tide maximum and the hydrograph. Tide–surge interactions can be largely explained by the fact that both phenomena affect the water depth and thereby the phase velocity of the tidal wave, the wind setup and the bottom friction. It was found that, as a result, a surge maximum is most likely to occur shortly after a low tide at most tide gauges along the UK and Dutch coasts [21,27], i.e., the phase shift between the surge maximum and the nearest high tide is usually not uniformly distributed. Another mechanism is the inverse proportionality of the wind setup to the water depth. This means that surges will be amplified in the case of low tides and reduced in the case of high tides, causing an oscillation in antiphase with the tide [27,28]. The effect of the tidal high on the surge maximum is, however, less pronounced. Williams et al. [29] could, for instance, not find any significant influence of the tidal high on the skew surge, simply because the effect of atmospheric variations is vastly larger than the minor variations in the average water depth. In contrast, Ragno et al. [30] and Diakomopoulos et al. [23] did find a negative dependence around the Italian and Dutch coasts, respectively.

It has been observed that extreme storm tides often show a tendency to cluster within a relatively short period of time [8,10,13]. The clustering of extreme storm tides usually results from the clustering of (moderate) extreme storm surges in combination with the spring tide [8]. The clustering of storms and storm surges is often associated with persistent large-scale meteorological and oceanographic conditions [31–33]. Another important mechanism is the secondary cyclogenesis, where secondary cyclones originate on the trailing fronts of parent (primary) cyclones [31,32,34]. Beside the serial clustering of storms, the harmonic behavior of tides and the seasonality of the weather may also favor some typical interarrival times. Haigh et al. [8], for example, found that a cluster of two extreme sea-level events is more likely to originate from two storm surge events when they are less than four days apart than when they are four to eight days apart. This is because, when the surges are four to eight days apart, one of them will happen during neap tide. Likewise, the strong seasonality in the storminess of Northwestern Europe favors storms clustering within the storm season.

Recently, Nieuwhuis [12] reported that about 25–30% of the storms (i.e., wind speed exceeding 20.8 m/s) at Hoek van Holland (close to the Maeslant Storm Surge Barrier, the Netherlands) may be considered a twin storm. This tendency to cluster also has a major impact on the clusters of closure events (CCEs) during which the Maeslant Storm Surge Barrier has to close two or more times in a short period. In 2017, Van den Brink and De Goederen [13] projected that two separate closure events within a week have a return period of 300 years and within a month 150 years. The study did not, however, include the effect of multi-closure events (MCEs) and did not assess the associated flood risk.

In this study, we investigate the statistics (severity and timing) and impact of multiple successive storm surge peaks that may require multiple closures of the Maeslant Storm Surge Barrier (MSSB) in a short period of time. First, we investigate the statistics of a cluster of multiple storm surge peaks resulting from different but related storms on the basis of the data analysis of a long record of sea level measurements at Hoek van Holland. Then, we assess the probability, severity and timing of a multi-closure event based on stochastic storm tide events that are currently used for the assessment and design of flood defenses in the Netherlands [35]. Finally, this information is used to assess the associated flood risk using the framework recently developed by Mooyaart et al. [15].

2. Maeslant Storm Surge Barrier (MSSB)

The Maeslant Storm Surge Barrier (MSSB) is a storm surge barrier located close to Rotterdam in the ‘Nieuwe Waterweg’ that protects over 1.5 million people against flooding.

The barrier consists of two 210 m wide and 17 m high floating sector gates that are closed in case of severe storm surges. In normal conditions, ships can pass through the barrier unimpeded as the gates are positioned in a dry dock on the side of the canal.

2.1. Water System

The MSSB is located in the Rhine–Meuse Delta where the river Meuse and two major distributaries of the river Rhine (Waal and Nederrijn/Lek) join together (Figure 1). The delta is characterized by two major outlets that are mutually interconnected by several smaller streams. The Nieuwe Waterweg–Scheur–Nieuwe Maas is the northern outlet in which the Maeslant barrier is located.

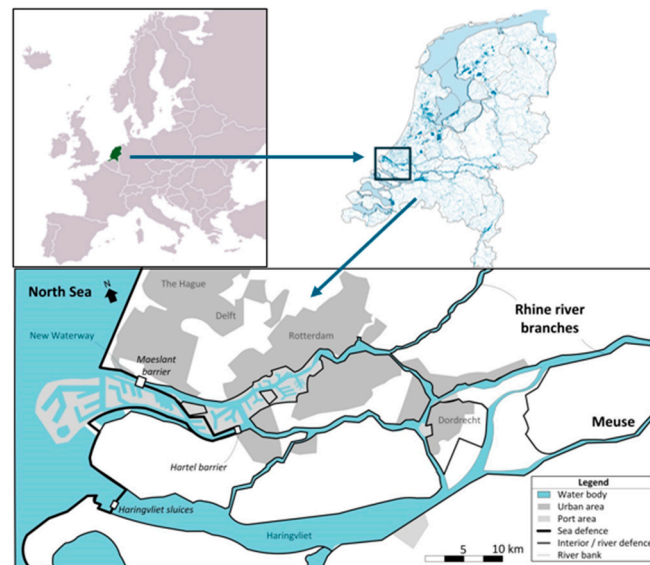


Figure 1. Overview of Rhine–Meuse Delta.

The Haringvliet is a former estuary that was closed by the Haringvlietdam in the seventies. The Haringvlietdam is a 5 km long dam that contains seventeen 56 m wide discharge sluices which regulate the water level and salinity in the Haringvliet. Around low tide, the gates are (partly) opened to freely discharge into the North Sea. During high tide, the sluices are only slightly opened to allow for fish migration and salt water intrusion, when there is sufficient river discharge from the Rhine and Meuse. Only in the case of severe storm surges are all of the gates fully closed. This operation practice reduces the tidal range of the Haringvliet to about 30 cm around MSL $\sim +0.5$ m.

2.2. Closing Procedure of Maeslant Barrier

The closing procedure of the MSSB starts when the water level at Rotterdam is predicted to exceed MSL + 3.0 m (or MSL + 2.9 m at Dordrecht). The operational team is mobilized, the barrier is prepared for operation and the start time of the actual closing is estimated. In case of moderate Rhine discharge, the barrier is closed when the water level at the barrier exceeds MSL + 2.0 m. When the Rhine discharge at Lobith exceeds 6000 m³/s, the barrier is closed at low water slack to create extra storage capacity.

A couple of hours before the actual closing, the dry dock is filled with water, the dock doors are opened and the drive system pushes the floating sector gates horizontally to the middle of the river. As the closing moment approaches, the sector gates are sunk down by letting water in. At the end of the surge, when the inner water level equals the outer water level again, the sector gates are floated up again by pumping the water out and are subsequently floated back into the dry docks.

After closing, the local water levels behind the MSSB are initially affected by different effects such as the negative translation wave behind the barrier and the tidal difference between the Nieuwe Maas and the Haringvliet [15]. These local effects are, however, relatively quickly averaged out after which the basin average water level increases more or less proportionally with the river inflow [36].

2.3. Closure Reliability

The Dutch Water Act dictates that the failure probability of a closure operation should be less than 1:100 per request [37]. In order to comply with this strict performance requirement, the storm surge barriers are maintained according to ProBO (Probabilistic Operations and Maintenance) [38]. This is a strict form of risk-based asset management based on a detailed reliability analysis. Nevertheless, even in case of a successful closure, it is plausible that the barrier becomes damaged during the operation [13,16] which may lead to a temporary reduction in its closure reliability. Potential damage of concern is often related to poorly understood oscillations during the lowering or lifting of the floating sector gates resulting in unanticipated rough landings on the sill, causing forces too large for the drive mechanism [16]. Such damage may easily require long repair times of several weeks or even up to a year.

3. Research Design

3.1. Model Strategy

The main objective of this study is to provide a first estimate of the potential impact of multi-peak storms and storm surge clusters on the performance of the Maeslant Storm Surge Barrier (MSSB). This is explored on the basis of a simple model framework that builds as much as possible on current practice in the Netherlands and the existing literature. Like Wong et al. [39], the different components of the framework are intentionally kept simple to promote the epistemic model values of accessibility, transparency, flexibility and efficiency.

3.2. Clusters of Closure Events (CCEs)

Storm tide clusters are defined as a series of storm tides from individual but related storms in a relatively short period of time. In this study, the interarrival time of two successive storm tides ($t_{a,stormtide}$) is defined as the time between the two successive storm tide peaks. Likewise, the interarrival time of two successive closure events ($t_{a,closure}$) is the time between the peaks of two successive closure events.

The probability density function of the interarrival time of two successive closure events pdf ($T_{a,closure} = t$) is estimated from a long randomly sampled record of storm surges (see Section 3.3.4), where the event maxima follow a Generalized Pareto Distribution (see Section 3.3.3) and the interarrival times $T_{a,stormtide}$, an empirical pdf (Section 3.3.2), are both estimated from a long observational data set of sea water levels at Hoek van Holland (Section 3.3.1).

3.2.1. Data and Selection of Storms

The CCE statistics are analyzed on the basis of a long sea water level record at Hoek van Holland (1953–2018) retrieved from the GESLA database version 3 [40] and homogenized by Diakomopolous et al. [23]. Like Diakomopolous et al. [23], we select all peaks above MSL + 212.2 cm. Yet, in contrast, no declustering time was applied because we were interested in clusters of extreme storm tides. In the case of storm tides with multiple peaks exceeding this threshold, only the highest peak was selected for further analysis. Two peaks that both exceed the threshold were considered to originate from two different storm surges if at least one of the peaks at the tidal highs in between is lower than MSL + 162.2 m

(50 cm lower than the threshold). If not, the peaks were assumed to belong to the same storm surge event and only the highest was selected for the analysis.

The selection of storm tide peaks is illustrated on the basis of the triplet storm Dudley, Eunice and Franklin that hit the Netherlands in February 2022 (Figure 2). The first storm, Dudley, did not generate water levels exceeding the selection threshold. The second storm, Eunice, was characterized by three peaks, of which only the second exceeded the selection threshold. After the third peak, the subsequent peak did not exceed the lower threshold and the selection algorithm therefore considers storm Eunice to have ended. Shortly thereafter, Franklin hit the coast with two peaks exceeding the threshold, of which only the largest was selected for further analysis.

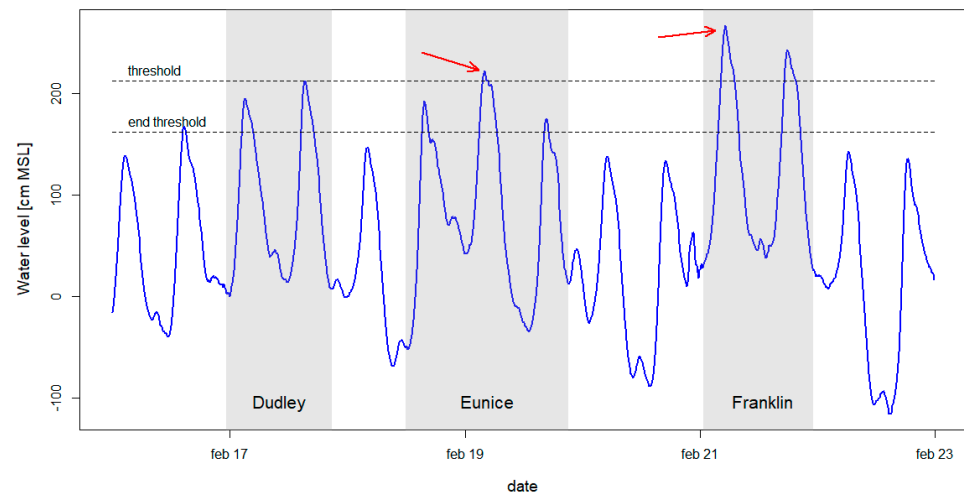


Figure 2. Example of the selection of sea water level peaks (indicated by red arrows) for the analysis of storm surge clusters (based on the triplet storm Dudley, Eunice and Franklin in February 2022).

This selection procedure resulted in 143 storm tide peaks in 65 years, i.e., a frequency λ of 2.2 per year. The selected storm tide peaks were used to estimate the empirical distribution of interarrival times and to perform extreme value analysis of the storm tide extremes.

3.2.2. Analysis of Clustering

The tendency to cluster was investigated by means of the interarrival times between the identified storm tide peaks. When the storm tide events are randomly distributed in time, the interarrival times would follow an exponential distribution with a failure frequency of $\lambda = 2.2 \text{ yr}^{-1}$. The deviation of the exponential distribution indicates that there is some kind of temporal pattern in the occurrence of the events. The overrepresentation of the short interarrival times (days to weeks) may indicate a tendency to cluster, whereas an underrepresentation of longer interarrival times (several months) may indicate that there is some kind of seasonality.

3.2.3. Extreme Value Analysis and Bias Correction

The Generalized Pareto Distribution (GPD) is fitted to the selected peaks using the R package *extRemes* [41]. It appears that the extreme data prepared by Diakomopoulos et al. [23] tend to be slightly lower than the official extreme statistics prepared for the safety assessment of the national flood defenses [35]. Therefore, a bias correction was applied to make the results more comparable to the current practice. This was achieved simply by adding a small value (i.e., the bias) to the selected peaks and applied threshold, such that the exceedance frequency of MSL + 300 cm equals 1:10 per year. Note that this bias correction does not change the scale and shape parameter.

3.2.4. Interarrival Times of Closure Events

The probability density function of the interarrival times of closure events pdf ($T_{a,closure} = t$) was estimated from a randomly sampled record of 100,000 storm tide peaks, of which the mutual interarrival times $t_{a,stormtide}$ were sampled from the empirical pdf ($T_{a,stormtide} = t$) (see Section 3.2.2) and the peak values from the Generalized Pareto Distribution (see Section 3.2.3). The cumulative sum of the interarrival times represents the time of occurrence with respect to time $t = 0$. From this record, all events exceeding the closure decision level (MSL + 300 cm) were selected and used to estimate the interarrival times between every pair of two successive closures. This subset of closure events was used to empirically estimate pdf ($T_{a,closure} = t$).

3.3. Multi-Closure Events (MCEs)

In this study, a multi-closure event (MCE) is defined as an extreme storm surge event during which the MSSB needs to close and open twice or more. Whereas the closing moment is solely determined by the outer water level h_{out} , the opening is started as soon the inner water level h_{in} equals the outer water level again. Therefore, the analysis of MCE needs to consider the time evolution of both the outer and the inner water level during the storm surge event.

The multi-closure events (MCEs) were analyzed by means of a slightly adapted stochastic storm tide event that was originally developed for the safety assessment of the Dutch primary flood defenses [35] and that was also used for a recently developed global data set of storm tide hydrographs [42]. A stochastic storm tide event describes the outer water level $h_{out}(t)$ at time t as the sum of the storm surge $h_{ss}(t)$ and the astronomical tide $h_t(t)$. In an open situation, the inner water level is assumed to equal the outer water level; when the MSSB is closed, the inner water level is modeled by a simple, calibrated reservoir model [36]. The statistics of the MCE are explored by means of a Monte Carlo simulation.

3.3.1. Stochastic Storm Surge Event

In this study, the evolution of the storm surge in time is described by a cosine-squared function because it was found that it describes the observed surges fairly well [27,43] and because it is relatively easy to implement.

$$h_{ss}(t) = h_{ss,mx} \times \cos^2(\pi \times t / T_{ss}) \quad (1)$$

In Equation (1), the stochastic variables $h_{ss,mx}$ and T_{ss} represent the storm surge maximum and duration, respectively. The extreme storm surge maxima $h_{ss,mx}$ are modeled by the Generalized Pareto Distribution (GPD) with a threshold of 107.6 cm, a shape parameter $\zeta = -0.062$ and a scale parameter $\sigma = 31.456$ [23]. The storm duration T_{ss} is described by a lognormal distribution with mean = 54.3 h and stdev = 18.8 h (i.e., $\mu_T = 3.938$ and $\sigma_T = 0.336$) [44].

3.3.2. Mutual Timing of Storm Surge and Tidal Peak

Following the advice of Geerse [27], we applied the full tidal variability rather than the average tide, as was achieved in the original framework [35]. We did this in the same manner as Diakomopoulos et al. [23], where we focus on tides in the year 2017.

The mutual timing of the surge events and tides is highly uncertain. The likelihood of a storm surge event occurring is subject to a strong seasonal cycle with a distinct peak in the winter months. The probabilities that a surge occurs within a certain month are estimated on the basis of the surge data prepared by Diakomopoulos et al. [23] by dividing all identified surges that occurred in a particular month by the total number of identified surges (Table 1).

Table 1. Relative share of total number of surges per month.

Month	Jan	Feb	Mar	Apr	May	Jun	Jul	Aug	Sep	Oct	Nov	Dec
Share	0.257	0.132	0.074	0.037	0.000	0.007	0.015	0.000	0.015	0.066	0.191	0.213

Within a monthly lunar cycle, the probability of the occurrence per unit time of a storm surge can be considered more or less constant. However, as mentioned before, storm surges may advance the tidal phase velocity. As a result, the phase difference φ between the surge maximum $t_{\text{surge,mx}}$ and the subdaily M2 tidal maximum $t_{\text{tide,mx}}$ usually appears not to be uniformly distributed [27]. For Hoek van Holland, we estimated a discrete distribution of the phase difference $\varphi = t_{\text{surge,mx}} - t_{\text{tide,mx}}$ based on surge and tide data prepared by Diakomopoulos et al. [23] (Table 2).

Table 2. Discrete distribution of phase difference $\varphi = t_{\text{surge,mx}} - t_{\text{tide,mx}}$ [hours].

φ	−6	−5	−4	−3	−2	−1	0	1	2	3	4	5	6
P	0.007	0.027	0.055	0.096	0.103	0.171	0.034	0.041	0.034	0.055	0.123	0.164	0.089

3.3.3. Inner Water Levels

When the barrier is closed, the water level is modeled by means of a simple, calibrated reservoir model, in a similar way to Zhong et al. [36]. For simplicity, it is assumed that the barrier closes instantaneously at $t = 0$ and that the water level is equally distributed over the subbasins shortly thereafter, i.e., the inner water level at the Maeslant barrier $h_{\text{in,MSSB}}$ equals the basin average inner water level $h_{\text{in,av}}$. Like Mooyaart et al. [15], the initial (average) water level directly after closing $h_{\text{in,av}}(0)$ is estimated at MSL + 100 cm. This is more or less the average water level of the Haringvliet and the Nieuwe Maas–Scheur. After closing, the inner water level $h_{\text{in,av}}$ will proportionally increase with the inflow from the three river branches Q_{rivers} divided by the area of the basin A_{basin} .

$$h_{\text{in,av}}(t) = h_{\text{in,av}}(0) + \left(\frac{Q_{\text{rivers}}}{A_{\text{basin}}} \right) t \tag{2}$$

Inflow under, through and over the barrier is not accounted for because this is usually dwarfed out by the river discharge and thus hardly affects the estimated MCE statistics. The effective area of the basin A_{basin} is estimated at 152 km² [36] and the inflow from the rivers is estimated from the discharge at Lobith ($Q_{\text{rivers}} = Q_{\text{Lobith}}$) where the river Rhine enters the Netherlands. In reality, only about 8/9 of Q_{Lobith} arrives at the Rhine–Meuse Delta, but the missing 1/9 is more or less compensated by the discharge from the Meuse river. Q_{Lobith} is described by a lognormal distribution with mean = 2502 m³/s and stdev = 1334 m³/s (i.e., $\mu_Q = 7.7$ and $\sigma_T = 0.5$) [15] and is considered completely independent from the storm surge during the surge [6].

3.3.4. Monte Carlo Simulation

A Monte Carlo simulation was performed with 524,000 random parameter samples (which is more or less the expected number of storm surge events in 100,000 years) to explore the frequency and characteristics of multi-closure events (MCEs). This number of samples was pragmatically chosen since this number requires only a limited simulation time (5 to 15 min on a normal laptop) whereas it is sufficient to provide robust estimates for events with the typical return periods of interest ($T \ll 10,000$ years).

The random samples consist of the storm surge maximum $h_{\text{ss,mx}}$, the storm surge duration T_{ss} , river discharge Q_{river} , the specific M2 tidal cycle (from 2017) that coincides

with the storm surge maximum, and the phase difference $\varphi = t_{\text{surge, mx}} - t_{\text{tide, mx}}$ between the surge and tidal peaks (Table 2).

Figure 3 illustrates how these parameters were used to simulate the outer and inner water level and MSSB operation. In this example, the surge (green line) has a maximum value of MSL + 284 cm and a duration of 71 h. The peak of the surge coincides with the M2 tidal cycle peaking on 15 January 2017 at 04:00:00, but has a phase difference ($\varphi = t_{\text{surge, mx}} - t_{\text{tide, mx}}$) of -4 h (gray shading). The summation of the surge (green line) and tide (blue line) results in the sea water level (black line). In this example, the sea water level exceeds the closure decision level (MSL + 300 cm) three times and the MSSB needs to close and open twice. Right after closing (at a level MSL + 200 cm), the inner water level (red) first equalizes with the average water level of the water basin (neglecting the inertia in the system). Subsequently, the basin is gradually filled by river inflow at a rate of $2700 \text{ m}^3/\text{s}$ until the inner water level equals the sea water level. At that moment, the MSSB is opened again.

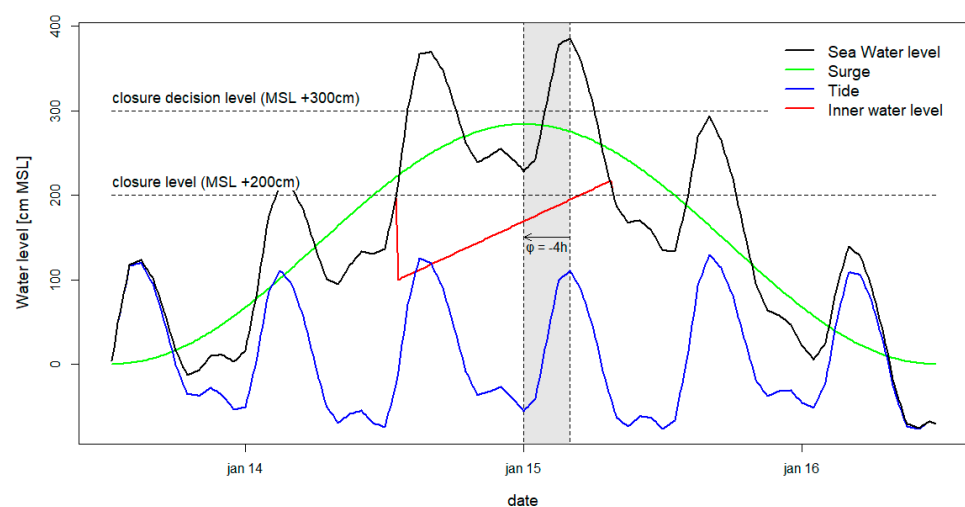


Figure 3. Example of simulation of multi-peak storm (MPS) with simplified stochastic storm event.

The outcomes of the 524,000 simulations are used to estimate the MCE statistics (frequency of single and double storm closure events and the distribution of the peak values during single- and double-closure events).

3.3.5. Bias Correction

Although the stochastic storm tide events apply calibrated values for the storm surge statistics, the phase shift and full tidal variation, the resulting extreme sea water level statistics may deviate from the official extreme statistics prepared for the safety assessment of the national flood defenses [35]. This bias might, for instance, be caused by the use of a storm surge hydrograph that is not fully representative of all storm surges. Therefore, a bias correction was applied to make the results more comparable to the current practice. This was achieved simply by multiplying the (exceedance) frequencies derived from the Monte Carlo analysis by a correction factor. This correction factor was chosen such that the exceedance frequency of MSL + 300 cm equaled 1:10 per year.

3.4. Flood Risk/Storm Surge Barrier Performance

The main function of a storm surge barrier is to reduce the extreme water level statistics behind the barrier. The difference between the extreme statistics with and without the barrier is referred to as the storm surge barrier performance [15]. This study extends on the analytical probabilistic procedure developed by Mooyaart et al. [15]. The influence

of multi-closure events (MCEs) and clusters of closure events (CCEs) is accounted for by adding two additional failure scenarios (Figure 4, blue scenarios).

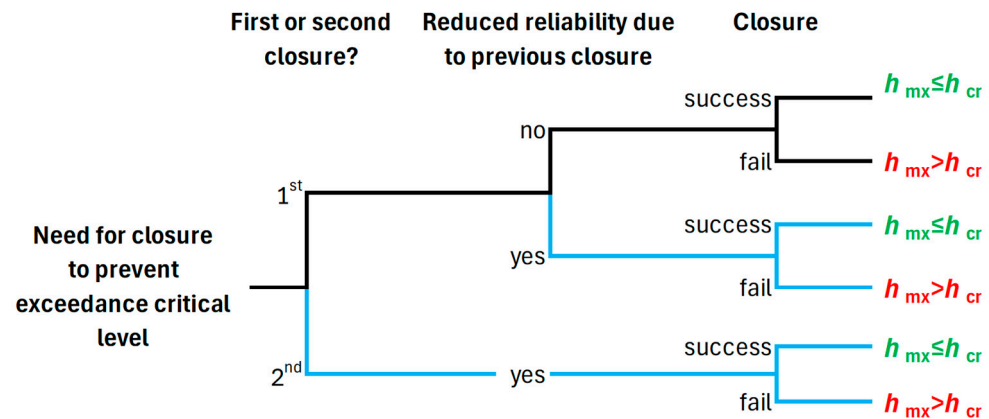


Figure 4. Event tree of failure scenarios for the assessment of storm surge barrier performance (blue scenarios are new with respect to Mooyaart et al. [15]).

For simplicity, structural failure and hydraulic overload are ignored since they appeared to have a minor influence on the exceedance probability of the critical water level of the interior flood defenses $h_{cr} = \text{MSL} + 3.60 \text{ m}$ [15].

3.4.1. Failure Scenarios

In this assessment, we consider three different types of closures (Figure 4): (1) an isolated (single or first) closure that was not preceded by another closure in the previous month (black scenario); (2) a preceded (single or first) closure that was preceded by another closure event in the month before; and (3) a second closure that was preceded by the first closure of the same multi-closure event. The isolated and preceded closure can be either a single-closure event or the first closure of a multi-closure event.

This leads to three scenarios that may lead to the exceedance of the critical inner water level $h_{cr} = \text{MSL} + 3.60 \text{ m}$ (Table 3).

Table 3. Failure scenarios for assessment of storm surge barrier performance derived from Figure 4.

Scenario	Event		Failure	
1	Isolated Closure	(IC)	Failed 1st closure	f _{ic}
2	Preceded Closure	(PC)	Failed 1st closure	f _{pc}
3	Second Closure	(SC)	Failed 2nd closure	f _{sc}

The exceedance frequency of the critical inner water level $F(h_{cr})$ is the sum of the exceedance frequencies of the three failure scenarios

$$F(H_{in,mx} > h_{cr}) = \sum_i^{n=3} F_i(H_{in,mx} > h_{cr}) \tag{3}$$

where $F_i(H_{in,mx} > h_{cr})$ refers to the exceedance frequency of h_{cr} due to failure scenario i that can be approached by (when neglecting structural failure and hydraulic overload) [15,45]

$$F_1(H_{in,mx} > h_{cr}) = F_{IC}(H_{out,mx} > h_{cr})P_{f,ic} \tag{4}$$

$$F_2(H_{in,mx} > h_{cr}) = F_{PC}(H_{out,mx} > h_{cr})P_{f,pc} \tag{5}$$

$$F_3(H_{in,mx} > h_{cr}) = F_{SC}(H_{out,mx} > h_{cr})P_{f,sc} \tag{6}$$

here, F_{IC} , F_{PC} and F_{SC} refer to the occurrence frequencies of outer water levels that without closure would lead to the exceedance of the critical inner water level due to an isolated closure (IC), a preceded closure (PC) and a second closure (SC), and $P_{f,IC}$, $P_{f,PC}$ and $P_{f,SC}$ refer to the failure probabilities of the isolated, preceded and second closure, respectively.

3.4.2. Probability of a Failed Closure

In accordance with Mooyaart et al. [15], we take the legally required failure probability of 1:100 per closure request [37] as the base failure probability regardless of the severity of the storm tide. This value is used as the probability of failure per request for isolated closures (ICs) that were not preceded by another closure in the month before ($P_{f,ic} = 0.01$).

For a second closure (SC) of a multi-closure event (MCE), there are both positive and negative effects on the failure probability ($P_{f,sc}$). The barrier recently closed, and given this success, it is unlikely that there is equipment under repair or subject to a dormant failure. Moreover, in between two closures belonging to the same multi-closure event, the sector gates are usually only floated up, but not moved back into the dry dock. In other words, the barrier is already in the correct horizontal position at the start of the second closure and only needs to be sunk down again. We expect that potential damage resulting from the first closure has a minor effect on the failure probability of the sinking procedure. Based on these considerations, we expect that the failure probability of the second closure (SC) of a multi-closure event (MCE) is between 1:1000 and 1:100 with an expected value of 1:200 ($P_{f,sc} = 0.005$).

For a preceded closure (PC) that was preceded by a closure resulting from another closure event, there are similar effects as with a second closure. However, the positive effects are smaller: there is more time in between the closures and the entire closure procedure needs to be redone. Potential major damage to the drive system and to the floating sector gates, resulting from the previous closure, may prevent the successful operation of the barrier. Given the poorly understood behavior of the sector gate in its floating position and the significant concerns about resulting major damage [16], this study assumes that the failure probability of an preceded closure (PC) is between 1:100 and 1:10 with an expected value of 1:20 ($P_{f,sc} = 0.05$).

3.4.3. Estimated Exceedance Frequencies

For the exceedance frequencies, we use the results from the analyses of the clusters of closure events (CCEs) and the multi-closure events (MCEs). We use the results of the CCE analysis to estimate the frequency of closure events $\lambda_{closure}$. The frequencies of the single- and double-closure events are estimated by multiplying the $\lambda_{closure}$ and the relative proportion of single and double closures as derived from the MCE analysis. Also, the conditional exceedance probabilities of single, first and second closures given a closure are derived from the MCE analysis.

4. Results

4.1. Clusters of Closure Events (CCEs)

4.1.1. Tendency to Cluster

The observed interarrival times between two successive storm tides show a clear tendency to cluster (Figure 5). Short observed interarrival times (red line) are overrepresented with respect to the theoretical case based on fully independent peaks (black line).

A large part of this clustering can be explained by the strong seasonality in the probability of the occurrence of extreme storm tides. In winter (especially in the months Nov–Feb) the probability of occurrence is much higher than in summer. Since there are on average 2.2 peaks per year that mainly occur in the four winter months, interarrival times

between 1 and 160 days are clearly overrepresented and interarrival times between 160 and 240 days are clearly underrepresented (gray line).

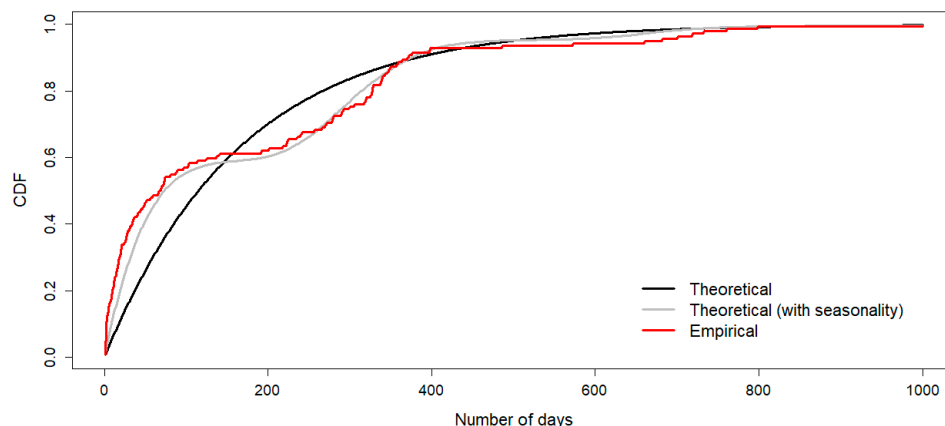


Figure 5. CDF interarrival times of storm surge events with sea water levels exceeding MSL + 212.2 cm.

Beside the seasonality, 13 out of the 142 pairs of successive peaks follow each other within two days. This is five times more than would be expected if there were no additional clustering on top of the seasonality (compare the large difference between the red and gray lines for short interarrival times).

4.1.2. Flood Frequency Analysis

The observed extremes are well described by the GPD (scale parameter 21.4 and shape parameter 0.033) (Figure 6). Without bias correction, however, the homogenized GESLA data tend to be slightly lower than the official extreme statistics prepared for the safety assessment of the national flood defenses (gray dots). Therefore, a bias correction of 18.3 cm was applied to the GESLA data (black dots) and threshold. In this way, the exceedance frequency of MSL + 300 cm according to the fitted GPD (red line) matches once in 10 years.

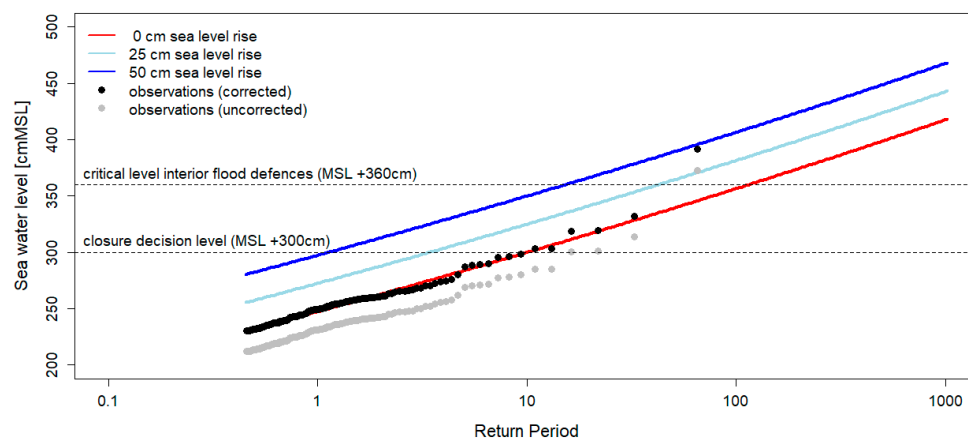


Figure 6. Return periods of extreme water levels at Hoek van Holland.

Sea level rise is accounted for in a similar way to the bias correction by adding the sea level rise to the applied threshold (blue lines).

4.1.3. Probability of Time Elapsed Since Previous Closure

According to the analysis, the probability that a storm closure is followed by a second closure within a month is about 2.3% (Table 4, column 2). This means that the probability

of two closures within a month is 1:435 per year. Given the clear tendency of storm surges to cluster, this probability may seem relatively low. This is, however, caused by the fact that only a small percentage (about 4.5%) of the storm surges require a closure. With sea level rise, the closure frequency, and thus the probability of a second closure within a short period of time, rapidly increases (Table 5, columns 3 and 4).

Table 4. Closure frequency and the probability of a second closure within certain time intervals.

Sea Level Rise	0 cm	25 cm	50 cm
Closure frequency	0.10	0.29	0.89
Probability that previous closure was within certain time:			
Two days	0.004	0.012	0.038
One week	0.009	0.024	0.072
One month	0.023	0.064	0.184

Table 5. Bias-corrected number of closure events per year simulated in 524,000 Monte Carlo experiments for different initial average inner water levels directly after closing, for current sea water level and with 25 cm and 50 cm sea level rises (SLRs).

SLR [cm]	h_{in} [cmMSL]	Number of Closure Events per Year				Proportion Double and Triple Closures
		Total	Single	Double	Triple	
0	100	0.10	0.09	0.008	0.001	9%
0	125	0.10	0.09	0.012	0.003	14%
0	150	0.10	0.08	0.014	0.004	18%
0	200	0.10	0.08	0.02	0.008	23%
25	100	0.23	0.20	0.02	0.004	11%
25	125	0.23	0.19	0.03	0.007	17%
25	150	0.23	0.18	0.04	0.011	21%
25	200	0.23	0.17	0.04	0.02	26%
50	100	0.53	0.46	0.06	0.013	14%
50	125	0.53	0.42	0.08	0.02	20%
50	150	0.53	0.40	0.10	0.03	25%
50	200	0.53	0.37	0.10	0.05	30%

4.2. Multi-Closure Events (MCEs)

Based on 524,000 Monte Carlo experiments (representative of ~100,000 years) with simplified stochastic storm tide events, it is estimated that there are on average 0.29 closure events per year (without bias correction). This closure frequency may be somewhat overestimated. According to the official statistics developed for safety assessments of the Dutch national flood defenses [35], the closure frequency is almost three times lower (~0.10 per year). This overestimation might be an artifact of the applied storm surge hydrograph. Although, the cosine-squared shape has been demonstrated to fairly well describe observed surges [27], it may overestimate the period of time during which the surge level is close to its maximum. In this way, the probability that a tidal high coincides with a surge level close to its maximum may be slightly overestimated, resulting in the overestimation of the exceedance frequencies.

This bias was corrected for by multiplying all simulated exceedance frequencies by a correction factor 0.34 (see Table 5).

The relative proportion of multi-closure events (last column) is hardly affected by sea level rise (first column), but substantially increases with increasing initial water level (second column). This is caused by the fact that a second closure is mainly associated with high inner water levels. A double closure event, i.e., the need to open and close the

barrier again between two tidal peaks, is only necessary if the inner water level exceeds the outer water level well before the end of the storm surge (see also Figure 2). This is mainly determined by the initial inner water level, river inflow and storm surge duration (Equation (2)). Sea level rise, storm surge height and tidal range also have some minor influence since they can slightly extend the duration of the closure. The dependence on storm surge height and tidal range makes double-closure maxima tend to be somewhat higher than single-closure maxima (Figure 7, blue line versus red line).

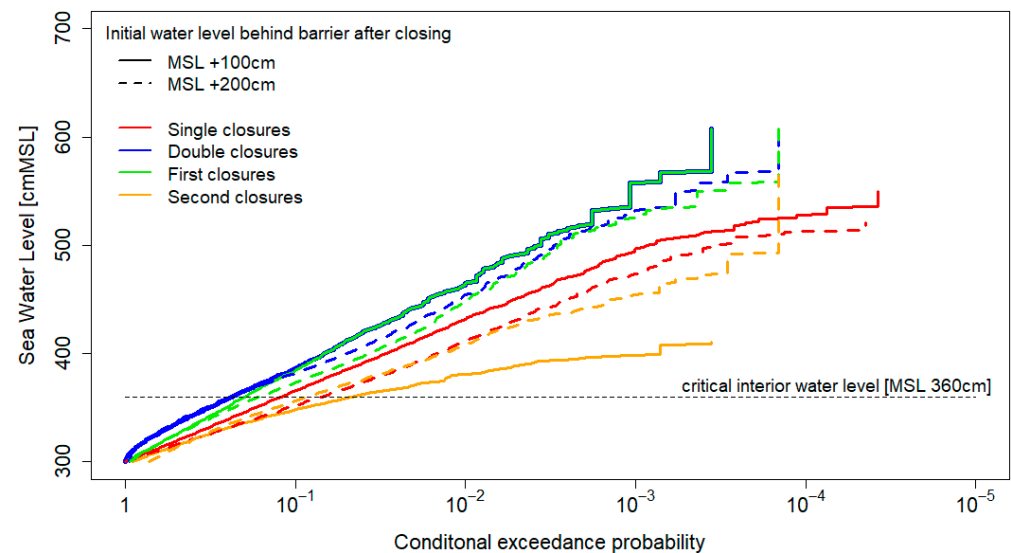


Figure 7. The conditional exceedance probabilities of the sea water level, given either a single- or a double-closure event.

Further, it appears that in about 2/3 of double closures, the first sea water level peak is higher than the second one. This results in substantially higher first closure maxima (green line) than second closure maxima (Figure 5, yellow line). As a result of the low initial inner water levels, opening the barrier is not always necessary during the first tidal low. Therefore, many first closures encompass two tidal peaks (see also the example in Figure 2). The second closure usually encompasses only one tidal peak, since the inner water level at the start of the second closure is usually much higher. Logically, the difference between first- and second-closure maxima rapidly decreases with increasing initial inner water levels (compare dashed yellow and green lines).

4.3. Storm Surge Barrier Performance

For the current situation, storm tide clusters hardly affect the extreme water level statistics behind the Maeslant Storm Surge Barrier (Figure 8). The exceedance probabilities of the critical water levels MSL + 300 cm and MSL + 360 cm only increase, respectively, from 1:1000 per year to 1:900 (upper bound 1:800) and from 1:7600 to 1:7000 (upper bound 1:6300). The influence of storm tide clusters is relatively minor because of the small probability that a closure event is preceded by another event in the month before (0.023). Yet, since the estimated failure probability of preceded closures is relatively high (0.05, with an upper bound of 0.1) some influence is detectable. The influence of multi-closure events is, however, almost negligible. This is the combined result of the relatively small number of events that require multiple closures (9%), together the relatively low estimated failure probability of second closures (0.005, with an upper bound of 0.01).

The relative contribution of storm surge clustering to flood risk rapidly grows with sea level rise (Figure 9), since sea level rise increases the probability of a preceding closure event (see Table 4). A sea level rise of 50 cm, for example, comes with an eight times higher

probability. When taking storm tide clustering into account, the projected exceedance frequencies of the critical levels MSL + 300 cm and MSL + 360 cm for 50 cm slr almost double, respectively, from 1:112 per year to 1:62 (with an upper bound of 40) and 1:827 per year to 1:487 (with an upper bound of 1:317). The influence of multi-closure events, however, also remains negligible with a 50 cm sea level rise. This is due to the fact that sea level rise only has a minor influence on the relative number of multi-closure events (see Section 4.2, Table 5).

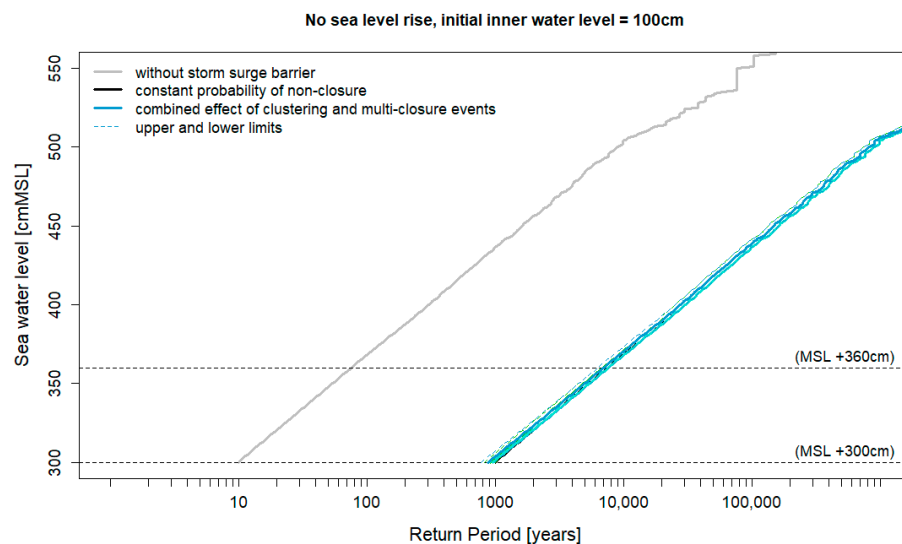


Figure 8. Return periods of extreme water levels in the inner basin behind the storm surge barrier for the current situation without sea level rise. The continuous lines represent the return periods of the system without the storm surge barrier (gray), with the storm surge barrier with a constant failure probability regardless of the type of closure event (black) and with the storm surge barriers taking into account multi-peak storms and storm surge clusters (dark blue), with lower and upper bounds (dashed lines).

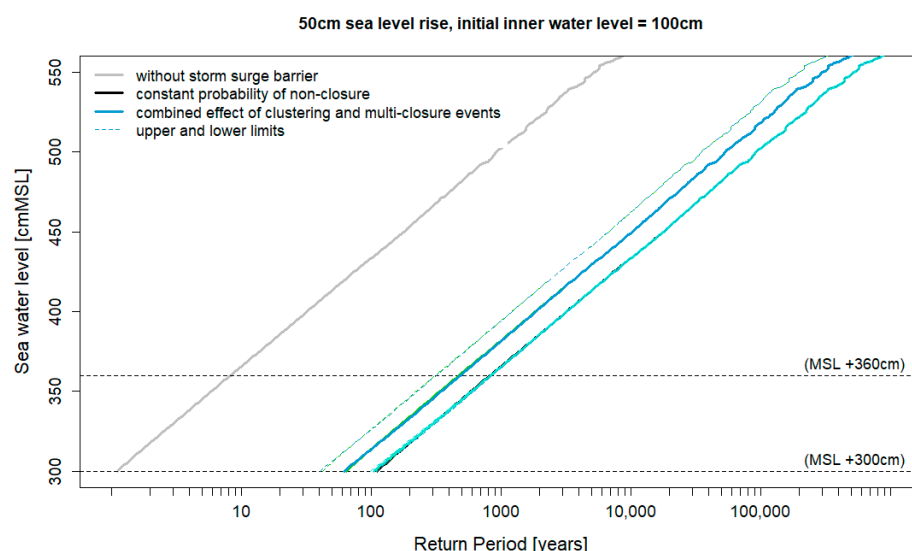


Figure 9. Return periods of extreme water levels in the inner basin behind the storm surge barrier for the current situation for 50 cm sea level rise. The continuous lines represent the return periods of the system without the storm surge barrier (gray), with the storm surge barrier with a constant failure probability regardless of the type of closure event (black) and with the storm surge barriers taking into account multi-peak storms and storm surge clusters (dark blue), with lower and upper bounds (dashed lines).

5. Discussion and Conclusions

This study investigated the statistics of multiple storm surge peaks in a relatively short period of time exceeding the closure decision level of the Maeslant Storm Surge Barrier at Rotterdam. Previous studies have shown that temporary compound events may substantially contribute to flood risk and that this is also the case for clusters of storm tide events at the MSSB. This research extends on previous studies by adding multi-peak storms and explicitly estimating the associated flood risk.

It was found that the main source of the clustering of closures of the Maeslant Storm Surge Barrier is seasonality. Because extreme storm tides tend to occur within a limited number of months, there is often little time between two successive extreme storm tide events when they occur within the same season. Even when they are mutually independent. Yet, in the current situation, the necessity of closing several times within a short time period barely contributes to the flood risk behind the MSSB. Sea level rise will however magnify this contribution. A sea level rise of 50 cm will increase the probability from 0.023 to 0.184 that a closure event is preceded by another closure less than one month before. Taking multi-peak storms and storm surge clusters explicitly into account almost doubles the projected probability of a failed closure from 1:112 to 1:62 per year for 50 cm sea level rise. This is especially due to the clusters of closure events.

The results are well in line with previous studies that suggested that compound events of moderate extremes may have a major impact on flood risk. It appears, however, that the results are highly sensitive to assumptions, model choices and the applied data, and therefore that the exact contribution to flood risk is highly uncertain. The projected probability of two closure events within a short time frame appears about three times lower than previously estimated by Van den Brink and De Goederen [10]. This is likely caused by a stronger temporal structure within the applied data generated by a surge model forced by long records of ECMWF seasonal forecasts. Likewise, the MCE analysis with standard storm patterns estimated closure frequencies three times too high by applying a more advanced representation of the astronomical tide, whereas the CCE analysis resulted in low closure frequencies three times too low by using a slightly different data set and homogenisation than are commonly used.

There are also some other limiting factors that may obscure the resulting risk estimates. First of all, the sensitivity of the operational reliability to storm closures is only a first rough estimate, not supported by data or structured expert judgment. Furthermore, the analysis was limited to double-peak storms not considering the possibility that storm events may also require three or even more closures. Additionally, other phenomena, like seiches, that may contribute to the multi-peak storm statistics were not considered. Finally, the study is limited to one type of compound event while others, for instance, the likely event that extreme storm surges co-occur with extreme wind conditions that may lower the operational reliability, were omitted.

Despite these limitations, the study clearly demonstrates the importance of considering a series of successive storm surge tide peaks in flood risk management. There are, however, also options to mitigate the additional flood risk. For instance, the frequency of double-peak storms could be lowered by lowering the water levels in the Haringvliet beforehand and closing the Maeslant barrier at low water slack. Alternatively, in the case of two expected peaks, of which the second is higher, it might be considered not to close at the first, i.e., accepting some flooding to reduce the probability of a big flood. The optimization of flood risk strategies requires a more elaborate risk analysis considering the limitations mentioned earlier.

Author Contributions: Conceptualization, A.M.R.B., D.L.T.R. and L.F.M.; methodology, A.M.R.B., D.L.T.R. and L.F.M.; software, A.M.R.B. and D.L.T.R.; validation, A.M.R.B. and D.L.T.R.; formal analysis, A.M.R.B.; investigation, A.M.R.B. and D.L.T.R.; data curation, A.M.R.B. and D.L.T.R.; writing—original draft preparation, A.M.R.B.; writing—review and editing, D.L.T.R. and L.F.M.; visualization, A.M.R.B.; supervision, A.M.R.B.; project administration, A.M.R.B. All authors have read and agreed to the published version of the manuscript.

Funding: This research received no external funding.

Institutional Review Board Statement: Not applicable.

Informed Consent Statement: Not applicable.

Data Availability Statement: The supporting R code can be downloaded at <https://github.com/alexanderbakker78/Clusters-of-storm-surge-barrier-closures> (accessed on 16 December 2024).

Acknowledgments: We gratefully acknowledge Faidon Diakomopoulos for his help with providing the data for our research.

Conflicts of Interest: Author Dion L. T. Rovers was employed by the company HKV Consultants. The remaining authors declare that the research was conducted in the absence of any commercial or financial relationships that could be construed as a potential conflict of interest.

References

- Green, J.; Haigh, I.; Quinn, N.; Neal, J.; Wahl, T.; Wood, M.; Eilander, D.; De Ruyter, M.; Ward, P.; Camus, P. Review Article: A Comprehensive Review of Compound Flooding Literature with a Focus on Coastal and Estuarine Regions. *EGU Sphere* **2024**. Preprint. [CrossRef]
- Eichentopf, S.; Karunarathna, H.; Alsina, J.M. Morphodynamics of sandy beaches under the influence of storm sequences: Current research status and future needs. *Water Sci. Eng.* **2019**, *12*, 221–234. [CrossRef]
- Zscheischler, J.; Martius, O.; Westra, S.; Bevacqua, E.; Raymond, C.; Horton, R.M.; van den Hurk, B.; AghaKouchak, A.; Jézéquel, A.; Mahecha, M.D.; et al. A typology of compound weather and climate events. *Nat. Rev. Earth Environ.* **2020**, *1*, 333–347. [CrossRef]
- Van den Hurk, B.J.J.M.; White, C.J.; Ramos, A.M.; Ward, P.J.; Martius, O.; Olbert, I.; Roscoe, K.; Goulart, H.M.D.; Zscheischler, J. Consideration of compound drivers and impacts in the disaster risk reduction cycle. *iScience* **2023**, *26*, 106030. [CrossRef] [PubMed]
- Van den Hurk, B.J.J.M.; Van Meijgaard, E.; De Valk, P.; Van Heeringen, K.-J.; Gooijer, J. Analysis of a compounding surge and precipitation event in the Netherlands. *Environ. Res. Lett.* **2015**, *10*, 035001. [CrossRef]
- Klerk, W.J.; Winsemius, H.C.; Verseveld, W.J.; Bakker, A.M.R.; Diermanse, F.L.M. The co-incidence of storm surges and extreme discharges within the Rhine–Meuse Delta. *Environ. Res. Lett.* **2015**, *10*, 035005. [CrossRef]
- Jane, R.; Cadavid, L.; Obeysekera, J.; Wahl, T. Multivariate statistical modelling of the drivers of compound flood events in south Florida. *Nat. Hazards Earth Syst. Sci.* **2020**, *20*, 2681–2699. [CrossRef]
- Haigh, I.D.; Wadey, M.P.; Wahl, T.; Ozsoy, O.; Nicholls, R.J.; Brown, J.M.; Horsburgh, K.; Gouldby, B. Spatial and temporal analysis of extreme sea level and storm surge events around the coastline of the UK. *Sci. Data* **2016**, *3*, 160107. [CrossRef] [PubMed]
- Jenkins, L.J.; Haigh, I.D.; Camus, P.; Pender, D.; Sansom, J.; Lamb, R.; Kassem, H. The temporal clustering of storm surge, wave height, and high sea level exceedances around the UK coastline. *Nat. Hazards* **2023**, *115*, 1761–1797. [CrossRef]
- Jenkins, L.J.; Haigh, I.D.; Kassem, H.; Pender, D.; Sansom, J.; Lamb, R.; Howard, T. Assessing the temporal clustering of coastal storm tide hazards under natural variability in a near 500-year model run. *Ocean. Dyn. Rev.* **2024**. Preprint, Version 1. [CrossRef]
- Ferreira, O. Storm Groups versus Extreme Single Storms: Predicted Erosion and Management Consequences. *J. Coast. Res.* **2005**, *SI*, 221–227. Available online: <https://www.jstor.org/stable/25736987> (accessed on 11 December 2024).
- Nieuwhuis, T.J.H. Modelling the Effect of Twin Storms on Dune Erosion. Master’s Thesis, Delft University of Technology, Delft, The Netherlands, November 2023. Available online: <https://repository.tudelft.nl/record/uuid:3730f825-7934-4c97-a4c2-473ca99fc39c> (accessed on 11 December 2024).
- Van den Brink, H.W.; De Goederen, S. Recurrence intervals for the closure of the Dutch Maeslant surge barrier. *Ocean Sci.* **2017**, *13*, 691–701. [CrossRef]
- Mooyaart, L.F.; Jonkman, S.N. Overview and Design Considerations of Storm Surge Barriers. *J. Waterw. Port Coast. Ocean Eng.* **2017**, *143*, 06017001. [CrossRef]

15. Mooyaart, L.F.; Bakker, A.M.R.; Van den Bogaard, J.A.; Jorissen, R.E.; Rijcken, T.; Jonkman, S.N. Storm surge barrier performance—The effect of barrier failures on extreme water level frequencies. *J. Flood Risk Manag.* **2025**, *18*, e13048. [CrossRef]
16. Rijkswaterstaat, Wettelijke Beoordeling Europoortkering I Dijktraject 208, version 2.2 Definitief, Netherlands; pp. 30–32. Available online: <https://waterveiligheidsportaal.nl/nss/assessment-lbo1> (accessed on 5 February 2025).
17. Walraven, M.; Vrolijk, K.; Kothuis, B.B. Chapter 20—Design, maintain and operate movable storm surge barriers for flood risk reduction. In *Coastal Flood Risk Reduction—The Netherlands and the U.S. Upper Texas Coast*, 1st ed.; Brody, S., Lee, Y., Kothuis, B.B., Eds.; Elsevier: Amsterdam, The Netherlands, 2022. [CrossRef]
18. Jonkman, S.N.; Merrell, W.J. Discussion of “Coastal Defense Megaprojects in an Era of Sea-Level Rise: Politically Feasible Strategies or Army Corps Fantasies”? *J. Water Resour. Plan. Manag.* **2024**, *150*, 07024002. [CrossRef]
19. Trace-Kleeberg, S.; Haigh, I.D.; Walraven, M.; Gourvenec, S. How should storm surge barrier maintenance strategies be changed in light of sea-level rise? A case study. *Coast. Eng.* **2023**, *184*, 104336. [CrossRef]
20. Wahl, T.; Mudersbach, C.; Jensen, J. Assessing the hydrodynamic boundary conditions for risk analyses in coastal areas: A stochastic storm surge model. *Nat. Hazards Earth Syst. Sci.* **2011**, *11*, 2925–2939. [CrossRef]
21. Horsburgh, K.J.; Wilson, C. Tide-surge interaction and its role in the distribution of surge residuals in the North Sea. *J. Geophys. Res.* **2007**, *112*, C08003. [CrossRef]
22. Ridder, N.; De Vries, H.; Drijfhout, S.; Van den Brink, H.; Van Meijgaard, E.; De Vries, H. Extreme storm surge modelling in the North Sea—The role of the sea state, forcing frequency and spatial forcing resolution. *Ocean Dyn.* **2018**, *68*, 255–272. [CrossRef]
23. Diakomopoulos, F.; Antonini, A.; Bakker, A.M.R.; Stancanelli, L.M.; Hrachowitz, M.; Ragno, E. Probabilistic characterizations of flood hazards in deltas: Application to Hoek van Holland (Netherlands). *Coast. Eng.* **2024**, *194*, 104603. [CrossRef]
24. Haigh, I.D.; Pickering, M.D.; Green, J.A.M.; Arbic, B.K.; Arns, A.; Dangendorf, S.; Hill, D.F.; Horsburgh, K.; Howard, T.; Idier, D.; et al. The tides they are a-changin’: A comprehensive review of past and future nonastronomical changes in tides, their driving mechanisms and future implications. *Rev. Geophys.* **2020**, *57*, e2018RG000636. [CrossRef]
25. Pugh, D.T. *Tides, Surges and Mean Sea Level (Reprinted with Corrections)*; John Wiley & Sons Ltd.: Chichester, UK, 1996; 486p.
26. Kew, S.F.; Selten, F.M.; Lenderink, G.; Hazeleger, W. The simultaneous occurrence of surge and discharge extremes for the Rhine delta. *Nat. Hazards Earth Syst. Sci.* **2013**, *13*, 2017–2029. [CrossRef]
27. Geerse, C. Interaction Between Tide and Surge—Modelling the Time Evolution of the Residual Surge. Report PR4366.10, HKV Consultants, The Netherlands. 2020. Available online: <https://open.rijkswaterstaat.nl/open-overheid/onderzoeksrapporten/@47126/interaction-between-tide-and-surge/> (accessed on 20 January 2025).
28. Barbot, S.; Pineau-Guillou, L.; Delouis, J.-M. Extreme storm surge events and associated dynamics in the North Atlantic. *J. Geophys. Res. Ocean.* **2024**, *129*, e2023JC020772. [CrossRef]
29. Williams, J.; Horsburgh, K.J.; Williams, J.A.; Proctor, R.N.F. Tide and skew surge independence: New insights for flood risk. *Geophys. Res. Lett.* **2016**, *43*, 6410–6417. [CrossRef]
30. Ragno, E.; Antonini, A.; Pasquali, D. Investigating extreme sea level components and their interactions in the Adriatic and Tyrrhenian Seas. *Weather. Clim. Extrem.* **2023**, *41*, 100590. [CrossRef]
31. Mailier, P.J.; Stephenson, D.B.; Ferro, C.A.T.; Hodges, K.I. Serial Clustering of Extratropical Cyclones. *Mon. Wea. Rev.* **2006**, *134*, 2224–2240. [CrossRef]
32. Pinto, J.G.; Gómara, I.; Masato, G.; Dacre, H.F.; Woollings, T.; Caballero, R. Large-scale dynamics associated with clustering of extratropical cyclones affecting Western Europe. *J. Geophys. Res. Atmos.* **2014**, *119*, 13704–13709. [CrossRef]
33. Priestley, M.D.K.; Pinto, J.G.; Dacre, H.F.; Shaffrey, L.C. The role of cyclone clustering during the stormy winter of 2013/2014. *Weather* **2017**, *72*, 187–192. [CrossRef]
34. Priestley, M.D.K.; Dacre, H.F.; Shaffrey, L.C.; Schemm, S.; Pinto, J.G. The role of secondary cyclones and cyclone families for the North Atlantic storm track and clustering over western Europe. *Q. J. R. Meteorol. Soc.* **2020**, *146*, 1184–1205. [CrossRef]
35. Chbab, H. *Basisstochasten WTI-2017—Statistiek en Statistische Onzekerheid, 1209433-012-HYE-0007*; Deltares: Delft, The Netherlands, 2016; Available online: https://publications.deltares.nl/1209433_012.pdf (accessed on 20 January 2025).
36. Zhong, H.; Van Overloop, P.-J.; Van Gelder, P.; Rijcken, T. Influence of a Storm Surge Barrier’s Operation on the Flood Frequency in the Rhine Delta Area. *Water* **2012**, *4*, 474–493. [CrossRef]
37. Dutch Water Act (Dutch: Waterwet). 2021. Available online: <https://wetten.overheid.nl/BWBR0025458/2021-01-01> (accessed on 20 January 2025).
38. Kharoubi, Y.; Van den Boomen, M.; Van den Bogaard, J.; Hertogh, M. Asset management for storm surge barriers: How and why? *Struct. Infrastruct. Eng.* **2024**, 1–15. [CrossRef]
39. Wong, T.E.; Bakker, A.M.R.; Ruckert, K.; Applegate, P.; Slangen, A.B.A.; Keller, K. BRICK v0.2, a simple, accessible, and transparent model framework for climate and regional sea-level projections. *Geosci. Model Dev.* **2017**, *10*, 2741–2760. [CrossRef]
40. Haigh, I.D.; Marcos, M.; Talke, S.A.; Woodworth, P.L.; Hunter, J.R.; Hague, B.S.; Arns, A.; Bradshaw, E.; Thompson, P. GESLA version 3: A major update to the global higher-frequency sea-level dataset. *Geosci. Data J.* **2023**, *10*, 293–314. [CrossRef]
41. Gilleland, E.; Katz, R.W. extRemes 2.0: An Extreme Value Analysis Package in R. *J. Stat. Softw.* **2016**, *72*, 1–39. [CrossRef]

42. Dullaart, J.C.M.; Muis, S.; De Moel, H.; Ward, P.J.; Eilander, D.; Aerts, J.C.J.H. Enabling dynamic modelling of coastal flooding by defining storm tide hydrographs. *Nat. Hazards Earth Syst. Sci.* **2023**, *23*, 1847–1862. [[CrossRef](#)]
43. Geerse, C.; Rongen, G.; Strijker, B. Schematization of Storm Surges—Analysis Based on Simulated KNMI-Data, Report PR3874.10. HKV Consultants, The Netherlands. 2019. Available online: <https://open.rijkswaterstaat.nl/open-overheid/onderzoeksrapporten/@222536/schematization-storm-surges-analysis/> (accessed on 20 January 2025).
44. Saman, K. Prestatiepeilenmodel Oosterscheldekering 2017, version 3.0 definitief. RWS Zee en Delta District Noord Oosterscheldekering, The Netherlands. 2017. Available online: <https://open.rijkswaterstaat.nl/open-overheid/@230297/prestatiepeilenmodel-oosterscheldekering/> (accessed on 20 January 2025).
45. Mooyaart, L.F.; Bakker, A.M.R.; Van den Bogaard, J.A.; Rijcken, T.; Jonkman, S.N. Economic optimization of coastal flood defence systems including storm surge barrier closure reliability. *J. Flood Risk Manag.* **2023**, *16*, e12904. [[CrossRef](#)]

Disclaimer/Publisher’s Note: The statements, opinions and data contained in all publications are solely those of the individual author(s) and contributor(s) and not of MDPI and/or the editor(s). MDPI and/or the editor(s) disclaim responsibility for any injury to people or property resulting from any ideas, methods, instructions or products referred to in the content.